Tony L. Schmitz
Jason E. Action
David L. Burris
John C. Ziegert
W. Gregory Sawyer

Department of Mechanical and Aerospace Engineering,
University of Florida,
Gainesville, FL 32611

Wear-Rate Uncertainty Analysis

Wear due to relative motion between component surfaces is one of the primary modes of failure for many engineered systems. Unfortunately, it is difficult to accurately predict component life due to wear as reported wear rates generally exhibit large scatter. This paper analyzes a reciprocating tribometer in an attempt to understand the instrument-related sources of the scatter in measured wear rates. To accomplish this, an uncertainty analysis is completed for wear-rate testing of a commercially available virgin polytetrafluoroethylene pin on 347 stainless steel counterface. It is found that, for the conditions selected in this study, the variance in the experimental data can be traced primarily to the experimental apparatus and procedure. Namely, the principal uncertainty sources were found to be associated with the sample mass measurement and volume determination.
[DOI: 10.1115/1.1792675]

1 Introduction

Engineered systems are subject to several modes of failure, including plastic deformation, fracture, fatigue, excess deflections, and wear. Of these, wear is generally the least predictable using current design methodologies. This is partially due to imperfect knowledge of the appropriate wear rate for the selected material pair to be used in calculating component life. Wear rate is normally determined experimentally using a tribometer, which attempts to mimic the contact conditions of the material pair and system under study. Wear-rate values reported in the literature for many material pairs and contact conditions often show wide variation, even for nominally identical tests. The source of this variation in measured wear rates is currently unknown. It may be due to actual variations in the wear rate of the material pair, or it may be due to intrinsic factors in the experimental apparatus and procedure that lead to variations in the reported wear-rate value. The purpose of this paper is to outline a method for determining the uncertainty of the measured wear rate for a given experimental apparatus as a function of the uncertainty of the measured input quantities and to compare the calculated measurement uncertainty with the experimental variance obtained using the apparatus. It is shown that the uncertainty analysis methodology reported here can also be used to determine the most significant contributors to the overall measurement uncertainty. This information can then be used to aid in redesign of the experimental apparatus and/or procedure to reduce the measurement uncertainty.

2 Wear Rate Measurement Description

2.1 Reciprocating Pin-on-Disk Tribometer. The tribometer shown schematically in Fig. 1 creates a reciprocating sliding contact between the two surfaces of interest. This tribometer is located inside a soft-walled clean room with conditioned air that has a relative humidity between 25 percent and 50 percent. A four-shaft pneumatic thruster, model 64a-4 produced by Ultramation,[1] creates the loading conditions of the contact using a 61.2 mm bore Bimba pneumatic cylinder. The cylinder is nominally protected from transverse loads by four 12 mm diameter steel rods. An electropneumatic pressure regulator controls the force produced by the thruster. The pneumatic pressure output is controlled using a variable voltage input in combination with an active control loop within the electropneumatic system. A linear positioning table is used to create the reciprocating motion between the stationary pin and counterface. The positioning system is composed of a table, ball screw, and stepper motor. Sliding speeds up to 152 mm/s are possible. The force created by the thruster and friction force generated by the contact is monitored using a six-channel force transducer. This load cell, which is mounted under the thruster, monitors forces created in the x, y, and z axes as well as the moments about these axes. The transducer output voltages are recorded using a data acquisition system (500 Hz sampling rate) and personal computer.

2.2 Experimental Procedure. Twenty-one wear-rate measurements for virgin polytetrafluoroethylene (PTFE) on 347 stainless steel were completed using nominally identical contacting conditions. The pin-sample preparation included computer numerically controlled machining of commercially available PTFE rod stock to a rectangular solid with dimensions of 6.35 mm $\times$6.35 mm$\times$12.7 mm. All samples were taken from the same rod of PTFE. Prior to testing, these samples were mounted in the sample holder, machined flat to the contacting surface, and the initial mass of the sample/holder was recorded. Wear tests are destructive by nature, and this preparation of a collection of nominally identical samples from a single source was felt to provide the most repeatable sample conditions. However, the variabilities in this sample preparation method are inherently embedded in the experiments. PTFE was chosen for this study because of its availability, low friction coefficient, high wear rate, and low sensitivity of its tribological behavior to the environment. Every effort was made to repeat nominally identical wear tests.

The 347 stainless steel counterface was prepared by wet-sanding with 600 grit sandpaper, cleaning with soap and water, and wiping with acetone and methyl alcohol prior to each test. All prepared counterface surfaces were examined using a scanning white-light interferometer to verify an average roughness R_a between 0.1 μm and 0.2 μm.

Testing was carried out for a predetermined number of cycles using a prescribed force level and reciprocating path. The average sliding speed was 73 mm/s and the average contact pressure was 4.3 MPa. The final sample/holder mass was then recorded, and the change in mass determined. Finally, the wear rate was calculated using the change in pin mass, initial pin dimensions and mass, force level, and total sliding distance.

3 Wear Rate Uncertainty Analysis

We define the measurand, or the specific quantity subject to measurement [1], as

$$K = \frac{V_L}{\overline{F}_n d} \tag{1}$$

where $V_L = \Delta m/\rho_S$ is the volume lost during the wear test, $\overline{F}_n$ is the average normal force (regulated to the desired value during

Contributed by the Tribology Division for publication in the ASME JOURNAL OF TRIBOLOGY. Manuscript received by the Tribology Division September 13, 2003; revised manuscript received March 18, 2004. Review conducted by: Q. Wang (Assoc. Ed.).

[1]Specific commercial equipment is identified to fully describe the experimental procedures. This identification does not imply endorsement by the authors.

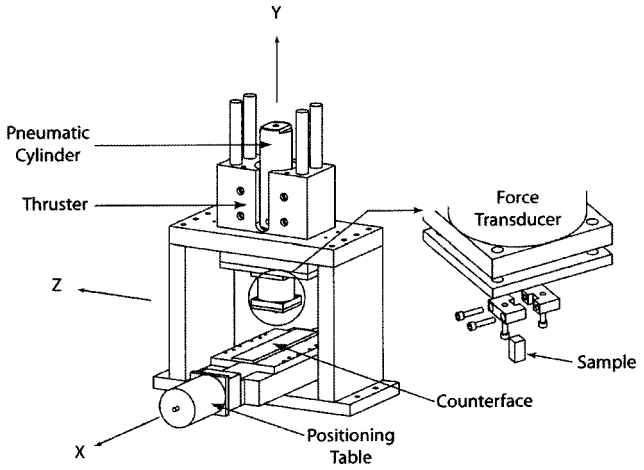

Fig. 1 Schematic of the reciprocating tribometer constructed for this study

testing), and $d=2SN$ is the total sliding distance. Also, Δm is the mass change in the sample due to wear, $\rho_S=m_i/V_S$ is the sample density, where m_i is the initial mass of the sample and $V_S=L_1L_2L_3$ is the initial volume of the rectangular solid sample (L_1, L_2, and L_3 are the lengths of the sides of the sample), S is the unidirectional sliding distance during each cycle, and N is the number of bidirectional cycles completed during the experiment. Substitution gives the following expression for the wear rate [2,3],

$$K=\frac{\Delta m L_1 L_2 L_3}{2\bar{F}_n m_i SN} \tag{2}$$

When reporting the wear-rate result, as with any measured quantity, it is also necessary to provide a quantitative statement regarding the quality of the reported value so that those who wish to use the data can have an indication of its reliability. The quantity that is used to characterize the ''dispersion of values that could reasonably be attributed to the measurand'' [1] is called the measurement uncertainty. The procedure used to determine the uncertainty of a measurement is referred to as an uncertainty analysis. Recommendations for carrying out uncertainty analyses are described in the International Standards Organization's *Guide to the Expression of Uncertainty in Measurement* [1] and the National Institute of Standards and Technology's *Guidelines for Evaluating and Expressing the Uncertainty of NIST Measurement Results*[2] [4]. The principles described in these documents are applied here.

For our measurements of wear rate, the measurand is not observed directly, but is determined from measurements of the individual input quantities Δm, L_1, L_2, L_3, $\bar{F}_n$, m_i, and S. Even after all known systematic error sources, or those that arise from a recognized effect, in these measurements have been evaluated and corrected or compensated, there still remains residual uncertainty in the reported result. An example of a systematic error that could occur in wear testing is an error in the manufacturer's reported value for the lead-screw pitch. If an encoder is used to record lead-screw rotations and the number of rotations is used to determine sliding distance, an error in the lead-screw pitch would introduce a bias into the computed sliding distance. If the manufacturer's value is known to be incorrect, the bias can be removed by measuring the lead-screw pitch directly to determine the value used for sliding-distance calculations. However, this pitch measurement and corresponding compensation will have some associated uncertainty, which must be included in the measurement uncertainty analysis.

[2]This document is available online at http://www.cstl.nist.gov/div836/836.01/PDFs/1994/TN1297.pdf.

In order to evaluate the measurement uncertainty, we can apply the *law of propagation of uncertainty* to determine the combined standard uncertainty u_c, which represents the estimated standard deviation σ, of the wear-rate measurement result. The combined standard uncertainty is a function of the standard uncertainty $u(x)$ of each input measurement and the associated sensitivity coefficients s, which are the partial derivatives of the functional relationship between the wear rate and input quantities with respect to each input quantity, as defined in Eq. (2). These partials are evaluated at nominal values of the input quantities. The expression for the square of the combined standard uncertainty in our wear-rate result is provided in Eq. (3),

$$\begin{aligned} u_c^2(K)=&\left(\frac{\partial K}{\partial \Delta m}\right)^2 u^2(\Delta m)+\left(\frac{\partial K}{\partial L_1}\right)^2 u^2(L_1)+\left(\frac{\partial K}{\partial L_2}\right)^2 u^2(L_2)\\ &+\left(\frac{\partial K}{\partial L_3}\right)^2 u^2(L_3)+\left(\frac{\partial K}{\partial \bar{F}_N}\right)^2 u^2(\bar{F}_n)+\left(\frac{\partial K}{\partial m_i}\right)^2 u^2(m_i)\\ &+\left(\frac{\partial K}{\partial S}\right)^2 u^2(S) \end{aligned} \tag{3}$$

where the standard uncertainty in each input variable can be determined using Type A or Type B uncertainty evaluations. In Type A evaluations, the standard uncertainty is set equal to the experimental standard deviation of the measured values (i.e., statistical methods are employed). Type B evaluations include all other methods, such as using engineering judgment or data supplied with a particular measurement transducer.

In Eq. (4), the partial derivatives in Eq. (3) have been evaluated. It should be noted that this equation does not contain the potential for correlation (or dependence) between the separate input variables (i.e., zero covariance has been assumed in this analysis, as is often the case)

$$\begin{aligned} u_c^2(K)=&\left(\frac{L_1L_2L_3}{2\bar{F}_n m_i SN}\right)^2 u^2(\Delta m)+\left(\frac{\Delta m L_2 L_3}{2\bar{F}_n m_i SN}\right)^2 u^2(L_1)\\ &+\left(\frac{\Delta m L_1 L_3}{2\bar{F}_n m_i SN}\right)^2 u^2(L_2)+\left(\frac{\Delta m L_1 L_2}{2\bar{F}_n m_i SN}\right)^2 u^2(L_3)\\ &+\left(\frac{-\Delta m L_1 L_2 L_3}{2\bar{F}_n^2 m_i SN}\right)^2 u^2(\bar{F}_n)+\left(\frac{-\Delta m L_1 L_2 L_3}{2\bar{F}_n m_i^2 SN}\right)^2 u^2(m_i)\\ &+\left(\frac{-\Delta m L_1 L_2 L_3}{2\bar{F}_n m_i S^2 N}\right)^2 u^2(S) \end{aligned} \tag{4}$$

In the following sections, we detail our evaluations of the standard uncertainties for the input quantities Δm, L_1, L_2, L_3, $\bar{F}_n$, m_i, and S. These values are then substituted into Eq. (4), with the partials evaluated at the nominal operating conditions for the testing carried out here, and the numerical value for the combined standard uncertainty is calculated (Section 3.6).

In many commercial, industrial, or regulatory applications, a measure of the uncertainty, which defines a measurement interval within which the measurand is confidently believed to lie, is desired. In this case, it is possible to report the expanded uncertainty U, which is the product of a coverage factor and the combined standard uncertainty. For a coverage factor of 2, for example, an interval is defined that has a confidence level of approximately 95 percent. For a coverage factor of 3, the confidence level is >99 percent. If the expanded uncertainty is used, it is necessary to report both the coverage factor and combined standard uncertainty.

3.1 Δm Standard Uncertainty. The mass change in the sample due to wear during the test is defined according to Eq. (5), where m_i is the initial mass and m_f is the final mass of the sample.

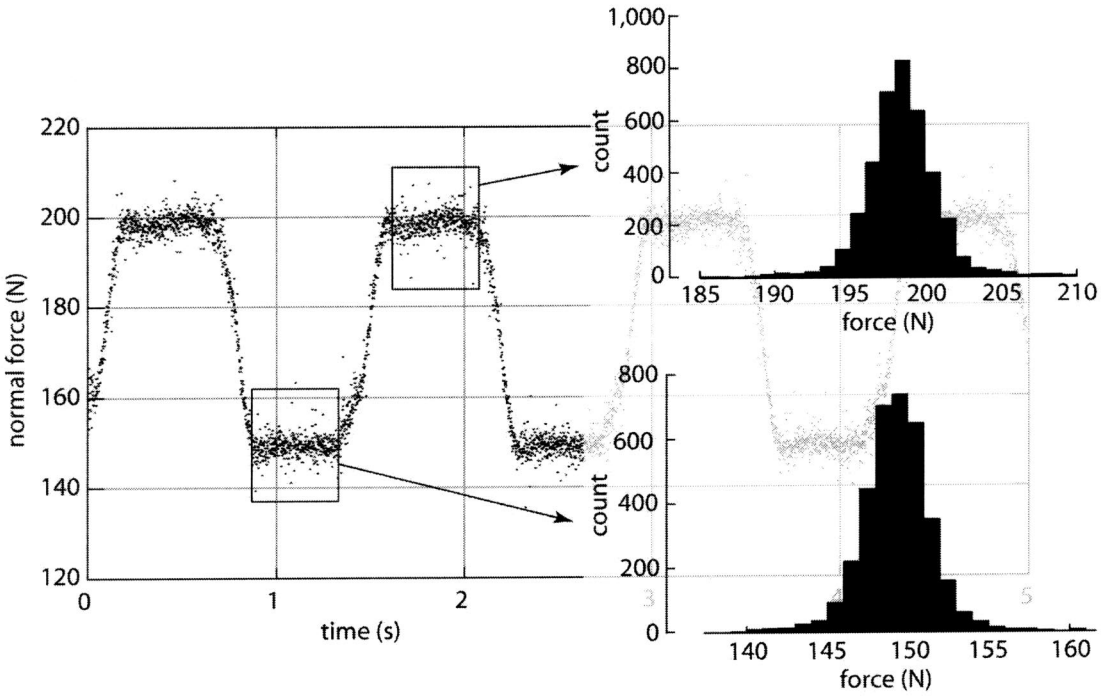

Fig. 2 Normal force versus time for PTFE on steel contact; histograms of the upper and lower normal forces are shown to the right

These values were recorded using an Ohaus Adventurer digital scale (model number AR3130). The scale has a resolution of 0.001 g (1 mg) and range of 310 g. The standard uncertainty in Δm is described using Eq. (6),

$$\Delta m = m_i - m_f \tag{5}$$

$$u^2(\Delta m) = \left(\frac{\partial \Delta m}{\partial m_i}\right)^2 u^2(m_i) + \left(\frac{\partial \Delta m}{\partial m_f}\right)^2 u^2(m_f) = u^2(m_i) + u^2(m_f) \tag{6}$$

Because m_i and m_f are nearly equal for the tests performed here (typical mass changes are on the order of a few percent), it is reasonable to assume that $u(m_f) \cong u(m_i)$ so that $u^2(\Delta m) = 2u^2(m_i)$. The manufacturer's data sheet provided with the mass scale lists a repeatability of 0.001 g, where repeatability is defined as the "closeness of the agreement between the results of successive measurements of the same measurand carried out under the same conditions of measurement" [1]. Repeatability is, therefore, fundamentally different from uncertainty and places an upper bound on the achievable accuracy. A conservative value of five times the repeatability is used for the scale's standard uncertainty, or $u(m_i) = 0.005$ g. The standard uncertainty in Δm is then $u(\Delta m) = \sqrt{2} \cdot 0.005 = 0.007$ g. Since we have chosen to use data supplied by the manufacturer to define $u(m_i)$, this is an example of a Type B uncertainty evaluation.

3.2 L_1, L_2, L_3 Standard Uncertainty. The rectangular wear block's dimensions prior to testing were recorded using a Mitutoyo digital caliper (model number SC-6). The instrument has a measuring range of 150 mm and a resolution of 0.1 mm. The manufacturer's specification for the instrument uncertainty was again available so we have used this value (Type B evaluation). The supplied value was 0.2 mm, and we have assumed that $u(L_1) = u(L_2) = u(L_3)$.

3.3 $\overline{F}_n$ Standard Uncertainty. A multiaxis force transducer manufactured by Advanced Mechanical Technology, Inc. (AMTI) was used to measure the normal force during the wear testing. As noted, the MC3A-6-500 is capable of measuring forces in the nominally orthogonal x, y, and z axes, as well as moments about these axes (see Fig. 1). This force transducer has a maximum load capacity of 2200 N along the y axis (vertical direction) and an 1100 N capacity in the x and z axes. Typical normal force data from our wear tests are shown in Fig. 2. It is seen that the normal force oscillates between maximum and minimum values with a normal (or Gaussian) distribution about each.

The normal force data oscillates at the same frequency as the commanded reciprocating motion between the PTFE sample and polished 347 stainless steel counterface. The cause of the normal force variation with motion direction has been studied and is believed to be due to compliance in the four linear bearings of the thruster unit, which allow the sample position to oscillate by several tens of micrometers when the motion direction changes. Despite this undesirable variation in normal force, the wear rate can be calculated according to Eq. (1), if the variation in the normal force is measured and accounted for in an appropriate manner. Because the recorded normal force is essentially bimodal, we have chosen to separate it into two bins, upper and lower, based on the direction of motion. The average force values for the upper and lower bins, $\overline{F}_u$ and $\overline{F}_l$, respectively, are calculated using Eq. (7),

$$\overline{F}_u = \frac{1}{n_u}\sum_{i=1}^{n_u} F_{u,i} \quad \overline{F}_l = \frac{1}{n_l}\sum_{i=1}^{n_l} F_{l,i} \tag{7}$$

where n_u and n_l are the number of samples in the upper and lower bins, respectively. The standard deviation in the mean values $\overline{F}_u$ and $\overline{F}_l$ are calculated according to Eq. (8) [5], where $s^2(F_u)$ and $s^2(F_l)$ are the squares of the standard deviations (i.e., variances) in the recorded values from the upper and lower bins, respectively.

$$u^2(\overline{F}_u) = \frac{s^2(F_u)}{n_u} = \frac{\dfrac{1}{n_u - 1}\displaystyle\sum_{i=1}^{n_u} (F_{u,i} - \overline{F}_u)^2}{n_u} \tag{8}$$

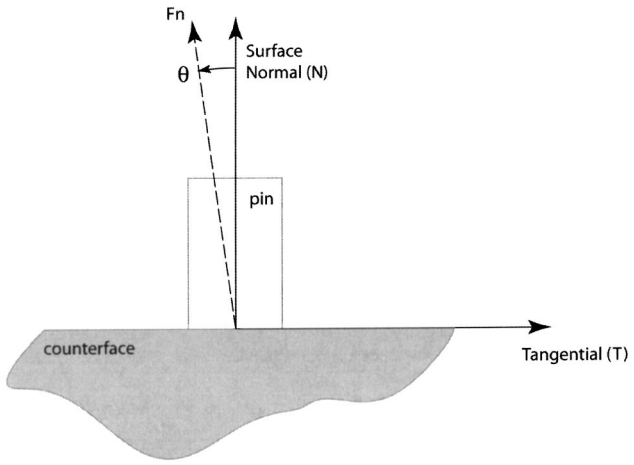

Fig. 3 Schematic of the cosine error in the normal force measurements

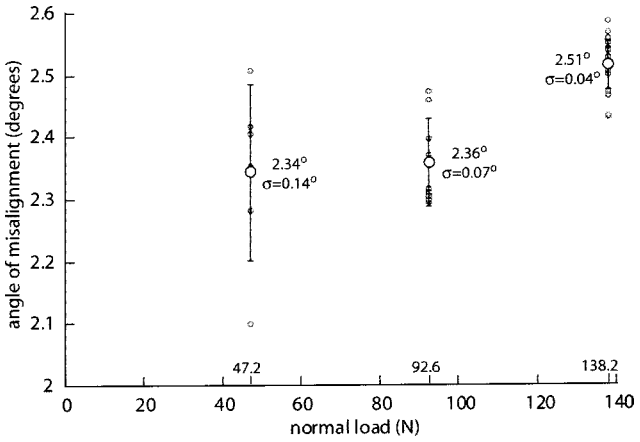

Fig. 4 Results from testing used to determine the angular misalignment illustrated in Fig. 3

$$u^2(\overline{F}_l)=\frac{s^2(F_l)}{n_l}=\frac{\frac{1}{n_l-1}\sum_{i=1}^{n_l}(F_{l,i}-\overline{F}_l)^2}{n_l}$$

The average normal force $\overline{F}_n$ is then calculated by

$$\overline{F}_n=\frac{\overline{F}_u+\overline{F}_l}{2} \tag{9}$$

From this relationship, the uncertainty in $\overline{F}_n$ is determined from

$$u^2(\overline{F}_n)=\left(\frac{\partial\overline{F}_n}{\partial\overline{F}_u}\right)u^2(\overline{F}_u)+\left(\frac{\partial\overline{F}_n}{\partial\overline{F}_l}\right)u^2(\overline{F}_l)=\frac{1}{4}[u^2(\overline{F}_u)+u^2(\overline{F}_l)] \tag{10}$$

The uncertainties of the average values from the upper and lower bins were determined to be 0.14 *N* and 0.15 *N*, respectively, using Eq. (8) (Type A evaluation). Substitution into Eq. (10) gives a standard uncertainty of 0.1 *N* for the average normal force of 175.0 *N*.

There is a second consideration in the normal force measurement uncertainty analysis, however. We must also treat the potential misalignment between the normal to the counterface surface and the force transducer axes. This misalignment leads to the familiar cosine error and is shown schematically in Fig. 3. In this case, the true (and unknowable) value of the normal force, $F_{n,true}$ is related to the measured normal force F_n through the secant of the misalignment angle θ as

$$F_{n,true}=\frac{F_n}{\cos\theta}=F_n\sec\theta \tag{11}$$

The result of this cosine misalignment is that the measured normal force is always less than the true normal force (i.e., a single-sided distribution of values). This introduces a bias into the recorded data that must be corrected. The reported value of the mean normal force $\overline{F}_{n,r}$ is therefore calculated as shown in Eq. (12), where $\overline{F}_{n,true}(1-\cos\theta)$, is the error introduced by the cosine misalignment, and we have substituted for $\overline{F}_{n,true}$ using Eq. (11)

$$\overline{F}_{n,r}=\overline{F}_n+\overline{F}_{n,true}(1-\cos\theta)=\overline{F}_n+\frac{\overline{F}_n}{\cos\theta}(1-\cos\theta)=\overline{F}_n\sec\theta \tag{12}$$

We must next calculate the standard uncertainty in this reported mean value; this will be the standard uncertainty substituted into the combined standard uncertainty calculation, rather than the result from Eq. (10). Again, we proceed by calculating the first-order Taylor series approximation to the measurement quantity as shown in Eq. (13),

$$u^2(\overline{F}_{n,r})=\left(\frac{\partial\overline{F}_{n,r}}{\partial\overline{F}_n}\right)u^2(\overline{F}_n)+\left(\frac{\partial\overline{F}_{n,r}}{\partial\theta}\right)u^2(\theta)=\sec^2\overline{\theta}\cdot u^2(\overline{F}_n)$$
$$+\sec^2\overline{\theta}\tan^2\overline{\theta}\cdot\overline{F}_{n,r}^2\cdot u^2(\theta) \tag{13}$$

Both the bias correction prescribed in Eq. (12) and the standard uncertainty shown in Eq. (13) require knowledge of the best estimate of θ. The angular misalignment for our test setup was determined by measuring the horizontal force produced from the application of a nominal normal force applied vertically. Any force that remained after the manufacturer-specified cross-talk had been removed was considered to be caused by misalignment. The mean angle of misalignment was calculated to be 2.45 deg from multiple repetitions under three different normal loads of 47.2, 92.6, and 138.2 *N*. The standard deviation of the measurement results, shown in Fig. 4, was 0.02 deg. We will assume the mean and standard deviation values obtained from this sample distribution provide the best estimates for the mean and standard deviation of the parent population. We can, therefore, substitute directly into Eq. (12) to determine the mean normal force value to be reported and Eq. (13) to obtain the standard uncertainty in this reported valued. These results are $\overline{F}_{n,r}=175.2$ N and $u(\overline{F}_{n,r})=0.2$ N.

3.4 m_i Standard Uncertainty. The standard uncertainty in the initial sample mass was defined in Section 3.1 as $u(m_i)=0.005$ g. The same value is used throughout this analysis.

3.5 *S* Standard Uncertainty. The positioning table, stepper motor, and controller used to produce the reciprocating motion of the contact was manufactured by Parker Automation. The linear positioning table (Model No. 406400XRMS) has a maximum stroke length of 400 mm. The ball screw that generates the table motion is driven by a RS33C stepper motor, which is actuated by a Zeta6108 controller. The commanded motion uncertainty reported in the manufacturer's data sheet was 0.041 mm. To verify this value, repeated attempts for a commanded motion of 50.8 mm were measured using an LVDT. All of the measured distances fell within a range of ± 0.295 mm. If we assume a uniform, or rectangular, distribution of the recorded values, the standard uncertainty is calculated as $0.295/\sqrt{3}=0.17$ mm [4]. We have conservatively selected to use this result because it is greater than the value reported by the manufacturer.

Similar to the normal force calculations in Sec. 3.3, we must consider a potential misalignment between the counterface surface and the sliding direction (see Fig. 5). In this case, the sliding

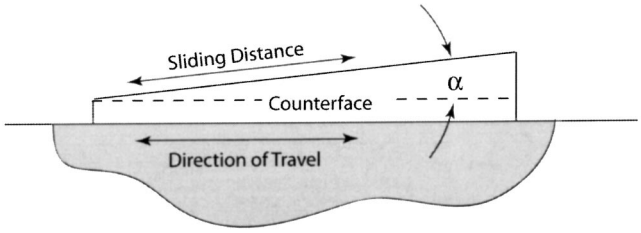

Fig. 5 Schematic of the counterface/sliding direction misalignment

distance along the counterface S will always be greater than the motion d_{table} imposed by the table for any angular misalignment. We can write the relationship between S and d_{table} as shown in Eq. (14), where α is the angle between the counterface and motion direction. The square of the standard uncertainty in S is shown in Eq. (15),

$$S = \frac{d}{\cos\alpha} = d_{\text{table}} \sec\alpha \tag{14}$$

$$u^2(S) = \sec^2\overline{\alpha}\cdot u^2(d_{\text{table}}) + \sec^2\overline{\alpha}\tan^2\overline{\alpha}\cdot\overline{d}^2_{\text{table}}\cdot u^2(\alpha) \tag{15}$$

In this case, we do not have a convenient method to measure the misalignment angle α. Therefore, we will assume that, although the most probable value of α is zero, its expected value $\overline{\alpha}$ is a small value of the same order as the uncertainty $u(\alpha)$ to which the counterface surface can be made parallel to the sliding direction. Under these assumptions, we will let α be described by $\overline{\alpha} \approx u(\alpha)$. Additionally, because the actual sliding distance is always greater than the commanded motion, the result is biased. The reported sliding distance s_r should, therefore, be $S_r = \overline{d}_{\text{table}}[1+\overline{u^2}(\alpha)]$ [6]. If we assume $\overline{\alpha} \approx u(\alpha) = 2$ deg $= 35$ mrad, $\overline{d}_{\text{table}} = 50.8$ mm, and $u(d_{\text{table}}) = 0.17$ mm, the resulting standard uncertainty in the sliding distance is 0.18 mm and the reported value is 50.86 mm.

3.6 Combined Standard Uncertainty. The combined standard uncertainty for our wear rate is calculated using Eq. (4). Table 1 summarizes the nominal values, standard uncertainties, and sensitivity coefficients for each input quantity. Substitution of the values provided in Table 1 into Eq. (4) gives a combined standard uncertainty of 7.4×10^{-5} mm^3/Nm. As a comparison, a Monte Carlo simulation was completed. In this simulation, each of the input parameters was varied about its mean value using the standard uncertainties provided in Table 1. Normal distributions were assumed for all input variables except the reported sliding distance, where a uniform distribution was applied. Example results for a total of 5×10^4 data points and 2600 cycles of motion (i.e., $N=2600$) are shown in Fig. 6. The simulated mean and standard deviation values are 5.05×10^{-4} mm^3/Nm and 7.4×10^{-5} mm^3/Nm. To help identify the most relevant uncertainty contributors, Table 2 lists, in descending order, the ratio of the standard uncertainty in each value to the mean value computed from the Monte Carlo simulation; these mean values are also included. To verify the combined standard uncertainty and Monte Carlo simulation results, we completed 21 single-point wear-rate measurements for PTFE on 347 stainless steel using nominally identical contacting conditions as described in Section 2.2.

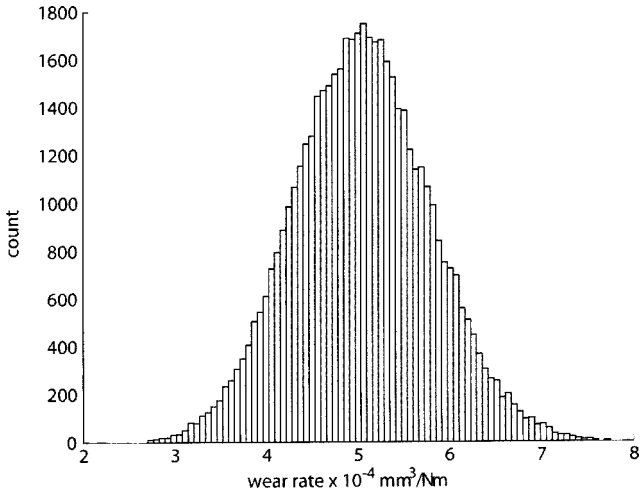

Fig. 6 Histogram from a 10,000 point Monte Carlo simulation using values taken from Table 1; the mean value was 5.05 $\times10^{-4}$ mm^3/Nm with a standard deviation of 7.4 $\times10^{-5}$ mm^3/Nm

A histogram of the experimental results is shown in Fig. 7. For the 21 experiments, the mean wear rate was found to be 5.04×10^{-4} mm^3/Nm and the standard deviation of the collected data was 6.0×10^{-5} mm^3/Nm. These results fall within the bounds predicted by the combined standard uncertainty and Monte Carlo simulation, which suggests that our analysis accounts for the primary uncertainty contributors in these wear-rate measurements.

4 Discussion

The results of the uncertainty analysis show that the overall uncertainty in the reported wear rate is dominated by the uncertainty in the measured mass change in the sample. This result is somewhat unexpected since the scale used for the measurements has a resolution of one milligram. Nonetheless, the uncertainty analysis shows that it likely accounts for approximately 91 percent of the observed variation in reported wear rate. Ultimately, this is because the mass of material lost due to wear is relatively small and the uncertainty of the scale is a large percentage of the sample mass change. A Monte Carlo simulation using realistic variances for the input quantities confirms the experimentally observed scatter in results. Therefore, one can see that in order to reduce the variance in the measurements, it is necessary to either

Table 1 Nominal values and standard uncertainties for PTFE on 347 stainless steel wear rate measurements

Input	Nominal Value	Standard Uncertainty, $u(x)$	Sensitivity, s	% Contribution $(s^2u^2(x)/u_c^2)$
Δm (g)	0.050	0.007	1.01065×10^{-2}	91
L_1 (mm)	30.8	0.2	1.64066×10^{-5}	0.2
L_2 (mm)	6.4	0.2	7.89568×10^{-5}	4.5
L_3 (mm)	6.4	0.2	7.89568×10^{-5}	4.5
$\overline{F}_{n,r}$ (N)	175.2	0.2	-2.88427×10^{-6}	0
m_i (g)	2.694	0.005	-1.87574×10^{-4}	0
S_r (m)	50.86×10^{-3}	0.18×10^{-3}	-9.93557×10^{-3}	0

Table 2 Ranking of uncertainty contributors from Monte Carlo simulation

Input	Mean Value	$u(x)$/Mean Value
Δm (g)	0.050	0.140
L_2 (mm)	6.4	0.031
L_3 (mm)	6.4	0.031
L_1 (mm)	30.8	0.007
S_r (m)	50.86×10^{-3}	0.004
m_i (g)	2.694	0.002
$\overline{F}_{n,r}$ (N)	175.2	0.001

perform much more accurate measurements of the mass change or wear away significantly more mass from the samples. Changes in almost any other part of the experimental apparatus/procedure will likely have little effect on the scatter of the experimental results.

Most materials undergo transient behaviors in wear during the early stages of sliding, often termed ''break-in'' or ''running-in.'' These early transient periods of wear are typically characterized by higher rates of material removal that eventually transition into a steady and nearly linear region of lower wear rate. This linear region is often termed the steady-state wear rate and is widely reported as the slope of a least-squares regression line through the data on a plot of the volume lost V_L versus the product of normal load $\overline{F}_n$, and sliding distance d $(\overline{F}_n d)$.

The previous analysis treated the uncertainty in calculating a wear rate from a single-point measurement of material removal and analytically propagated the individual uncertainty contributors. The analytical treatment of the uncertainty in the steady-state wear rate computed from multiple interrupted measurements (i.e., the slope of the least-squares regression line though multiple data points) is cumbersome. However, a Monte Carlo model can be developed that accounts for the measurement input uncertainties described in Sections 3.1–3.4 while carrying out many least-squares regressions. The mean slope (wear rate) and standard deviation in slope from the Monte Carlo model can then be used as estimates of the mean wear rate and associated uncertainty [7].

Therefore, we carried out a 1000 iteration simulation to determine the steady-state wear-rate uncertainty. This simulation, similar to the one described in Section 3.6, varied each of the input parameters about the mean values using assumed distributions and calculated 1000 different slopes on a V_L versus $\overline{F}_n d$ plot. The average of these calculated slopes is reported as the mean steady-state wear rate and the standard deviation is taken to be the associated uncertainty.

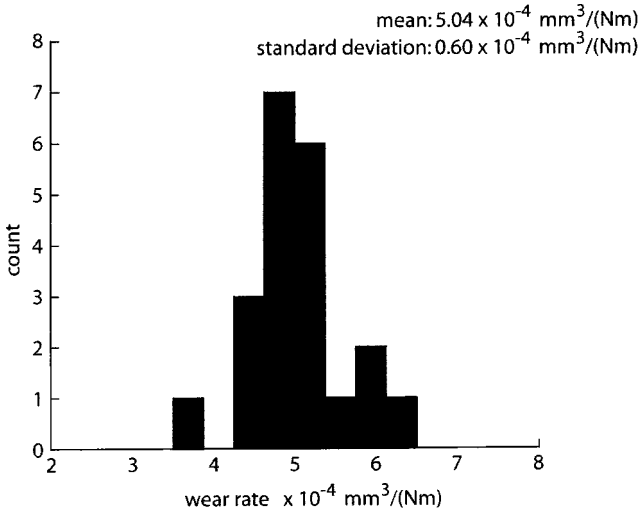

Fig. 7 Histogram from 21 experiments with PTFE on stainless steel; the mean value was $K=5.04\times10^{-4}$ mm^3/Nm with a standard deviation of 6.0×10^{-5} mm^3/Nm

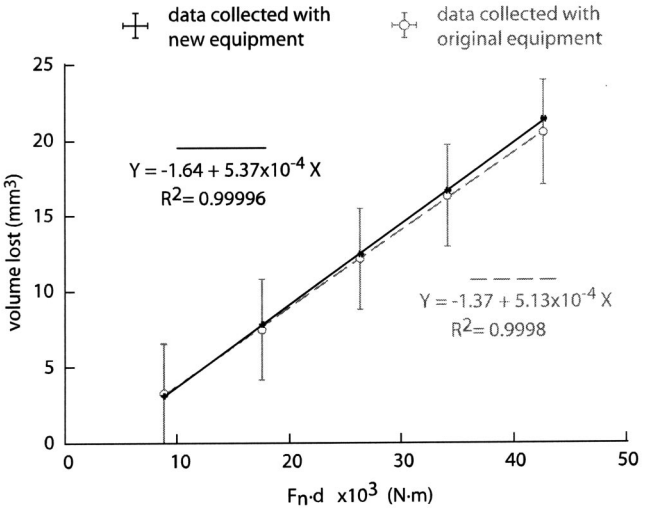

Fig. 8 Interrupted wear-rate measurement results are shown; the light gray open circles and associated error bars correspond to measurements completed using the original scale and calipers; black error bars and regression line represent data gathered using the new scale and micrometer. The error bars in the vertical and horizontal directions are plotted in each case, but some cannot be observed at the plot scale. Using the new equipment, the caps on the error bars are longer than the bars themselves.

To test the validity of this Monte Carlo approach, a single test of PTFE on 347 stainless steel was completed under the same conditions as reported previously. Unlike the previous experiments, however, this test was interrupted every 480 cycles and measurements of mass loss were made. The individual data points are shown in Fig. 8 by the open circles. The error bars shown on this plot were calculated according the analytical approach discussed in Sections 3.1–3.4. The Monte Carlo simulation gave a mean wear rate of $K=5.08\times10^{-4}$ mm^3/Nm and an uncertainty of $u(K)=1.24\times10^{-4}$ mm^3/Nm. This is in excellent agreement with the previous data, although the Monte Carlo simulation gives a larger uncertainty than the previous analysis because the uncertainties in the starting points are also included in the fitting (i.e., in a single-point wear-rate test, it is implicitly assumed that the data extrapolates perfectly through the origin).

Prior to performing these interrupted experiments, a new scale (Mettler Toledo AX 205) and a new micrometer (Brown & Sharpe Micromaster mm 2000) with resolutions of 0.01 mg and 0.001 mm, respectively, were purchased. Standard uncertainties in measurements completed with these two instruments represented over 90 percent of the final combined standard uncertainty in the previous analytic treatment. Again, we selected to conservatively assume a standard uncertainty of five times the instrument resolution in both cases (standard uncertainty values were not provided by the manufacturers). Even under these conservative conditions, the new equipment still provided a greater-than-ten-times reduction in the combined standard uncertainty over the previous scale/caliper combination (because these instruments were purchased after the 21 single-point measurements were completed, we were unable to verify the expected reduction in data scatter). The filled circles in Fig. 8 represent measurement results for the same sample during the interrupted wear rate testing using the new equipment. As expected, these values fall within the uncertainty bounds determined from the original equipment. Also, a weight dependent bias in the original scale was observed. The Monte

Carlo simulation for the measurements using the new scale and micrometer gives a wear rate of $K = 5.37 \times 10^{-4}$ mm^3/Nm and an associated uncertainty of $u(K) = 2.63 \times 10^{-6}$ mm^3/Nm.

5 Conclusions

In this work we have completed uncertainty analyses for single-point and steady-state wear-rate measurements for virgin polytetrafluoroethylene (PTFE) on 347 stainless steel using a reciprocating tribometer. Both analytic and Monte Carlo methods were applied to determine the relative importance of the individual uncertainty contributors, including sample mass and size, sliding distance, and normal force. Through these analyses, it was found that the primary sources of uncertainty were mass-change measurements and length measurements of the sample for the testing conditions selected for this study. While the standard uncertainty values used will not apply, in general, to other experimental equipment and material pairs, we have provided a general framework for carrying out uncertainty analyses on wear rate measurements. Our analysis focused on the instrument-related uncertainty contributors for three reasons: 1) the instrument-based uncertainty must be known before perturbation levels for process parameters that are not well understood can be established, 2) the material pair was chosen to minimize the influence of environmental contributions, and 3) sample preparation was carefully completed to reduce experimental variation from one test to another.

The completion of an uncertainty analysis to determine confidence in the measured data is particularly important in wear rate testing because there is no convenient artifact which can be used to compare the performance of different instruments. Since the sample is destroyed during testing and it is difficult to exactly reproduce the counterface (not to mention variations in environmental conditions), it is not possible to test two instruments under exactly the same circumstances. In this case, a defensible uncertainty analysis offers the only reasonable means to compare the performance of two or more tribometers.

Acknowledgments

This material is based on work supported by the National Science Foundation under Grants No. CMS-0219889 and No. DMI-0238019. Any opinions, findings, and conclusions or recommendations expressed in this material are those of the authors and do not necessarily reflect the views of the National Science Foundation. The authors would like to acknowledge valuable discussions regarding the normal force uncertainty with Dr. A. Davies, University of North Carolina-Charlotte. Additionally, the cosine uncertainty in Section 3.5 follows the analysis outlined by Dr. W. T. Estler, National Institute of Standards and Technology, in Ref. [6].

References

[1] International Standards Organization (ISO), 1993, Guide to the Expression of Uncertainty in Measurement (Corrected and Reprinted, 1995).

[2] Archard, J. F., 1953, "Contact and Rubbing of Flat Surfaces," J. Appl. Phys., **24**, pp. 981–988.

[3] Meng, H. C., and Ludema, K. C., 1995, "Wear Models and Predictive Equations: Their Form and Content," Wear, **181–183**, pp. 443–457.

[4] Taylor, B. N., and Kuyatt, C. E., 1994, "Guidelines for Evaluating and Expressing the Uncertainty of NIST Measurement Results," NIST Tech. Note 1297.

[5] Bevington, P. R., and Robinson, D. K., 1992, *Data Reduction and Error Analysis for the Physical Sciences*, 2nd Ed., McGraw-Hill, Boston, MA.

[6] Schmitz, T. L., Evans, C. J., Davies, A., and Estler, W. T., 2002, "Displacement Uncertainty in Interferometric Radius Measurements," CIRP Ann., **51**(1), pp. 451–454.

[7] Hazelrigg, G. A., 1996, *Systems Engineering: An Approach to Information-Based Design*, Prentice-Hall, Upper Saddle River, NJ.